THE RELATIONSHIP BETWEEN STELLAR AND BLACK HOLE MASS IN SUBMILLIMETER GALAXIES

C. BORYS

Department of Astronomy, California Institute of Technology, Pasadena, CA 91125; borys@caltech.edu

IAN SMAIL

Institute for Computational Cosmology, Durham University, South Road, Durham DH1 3LE, UK

S. C. CHAPMAN AND A. W. BLAIN

Department of Astronomy, California Institute of Technology, Pasadena, CA 91125

D. M. ALEXANDER

Institute of Astronomy, University of Cambridge, Madingley Road, Cambridge CB3 0HA, UK

AND

R. J. IVISON[1]

Astronomy Technology Centre, Royal Observatory, Blackford Hill, Edinburgh EH9 3HJ, UK

ABSTRACT

We analyze deep X-ray, optical, and mid-infrared *Spitzer* observations of the CDF-N/GOODS-N region to study a sample of 13 submillimeter-detected galaxies with spectroscopic redshifts (median $z = 2.2$). These galaxies are among the most active and massive at this epoch. We find evidence for a power-law correlation between the estimated stellar and X-ray luminosity, implying that masses of the black holes may be related to the stellar masses of their host galaxies. We derive the rest-frame UV–near-infrared spectral energy distributions for these galaxies, believed to be young spheroids, and fit them with model templates. Using the rest-frame near-infrared luminosities, which are relatively insensitive to uncertainties in stellar ages and reddening in these young dusty galaxies, and theoretical mass-to-light ratios, we can estimate their stellar masses. Although the submillimeter emission implies that these galaxies are undergoing an epoch of intense star formation, the *Spitzer* data reveal a massive stellar population already in place. We find that our submillimeter galaxies have a median stellar mass of $\sim 10^{11} \, M_\odot$, which is roughly 10 times more massive than typical UV-selected star-forming systems at similar redshifts. These stellar masses are then compared to previously published black hole mass estimates derived from the X-ray luminosities under the assumption of Eddington-limit accretion. We find that the black hole masses for our high-redshift sample are approximately 1–2 orders of magnitude smaller than galaxies of comparable stellar mass in the local universe. Although our estimates of black hole masses will increase if the accretion is sub-Eddington, and our stellar masses will decrease if we assume a much younger stellar population or a different initial mass function, we find that only through a combination of effects is it possible to shift the high-redshift galaxies such that they lie on the local relation. This suggests that the black holes need to grow substantially between $z = 2.2$ and the present day, with much of the black hole growth occurring *after* the current obscured, far-infrared luminous phase of activity, which is likely associated with the formation of the spheroid. This interpretation supports a scenario in which submillimeter galaxies pass through a subsequent accretion-dominated phase, where they would appear as optically bright quasars.

Subject headings: galaxies: evolution — galaxies: formation — galaxies: high-redshift — galaxies: starburst

Online material: color figures

1. INTRODUCTION

Studies of galaxies in the local universe have demonstrated an apparent relation between the stellar mass of a spheroid and that of the supermassive black hole (SMBH) that lies at its heart. The $M_\star$-$M_{\rm BH}$ relation for spheroids, with the mass of the SMBH typically $\sim 0.1\%$ of the spheroid mass (e.g., Kormendy & Richstone 1995; Magorrian et al. 1998; Gebhardt et al. 2000), suggests that the growth of the black hole and the surrounding galaxy are related. This provides an important clue to understanding galaxy formation, as SMBHs have been suggested as a highly efficient mechanism for regulating star formation in galaxies (e.g., Cavaliere & Vittorini 2002; Granato et al. 2004; Di Matteo et al. 2005). Such *feedback* is an essential part of current galaxy formation models

and provides a physically motivated explanation for the form of the galaxy luminosity function (Benson et al. 2003; Baugh et al. 2005). However, observational evidence for feedback, in particular driven by activity from SMBHs, is sparse, especially for the youngest and most massive galaxies—for which it is expected to be most important (Benson et al. 2003).

Modeling AGN-driven feedback is more difficult than the traditional star formation feedback recipes. In part this is because we still lack a clear model for the early growth of the SMBH, where BH-BH mergers and super-Eddington accretion may both play a part. There is thus an urgent need for observations of the earliest phases of the evolution of spheroids and SMBHs to guide development of theoretical models.

Studies of the submillimeter galaxy (SMG) population (e.g., Smail et al. 1997, 2002; Barger et al. 2000; Ivison et al. 2002; Webb et al. 2003; Borys et al. 2004; Wang et al. 2004; Greve et al. 2004) suggest that luminous far-infrared galaxies are likely to be

associated with an early phase in the formation of massive galaxies. The intensity of their starbursts and the resulting high metallicity, along with their large dynamical masses, high gas fractions, and strong clustering (Ivison et al. 2002; Greve et al. 2005; Swinbank et al. 2004; Blain et al. 2004), are all suggestive of a close link to the formation phase of the most massive spheroids (Smail et al. 2004). If these are indeed young spheroids, what can we learn about their black holes?

Deep X-ray observations provide a sensitive probe of AGN activity in SMGs and can be used to place SMBH mass constraints, even in the presence of heavy gas and dust obscuration. Exploiting the unique sensitivity of the 2 Ms exposure of the Chandra Deep Field–North (CDF-N; Alexander et al. 2003), Alexander et al. (2005a, 2005b) study a small sample of *spectroscopically identified* SMGs and find that most host weak AGNs with modest absorption-corrected X-ray luminosities. This suggest two things: (1) the AGNs do not typically dominate the bolometric emission from SMGs, and (2) the masses of the SMBHs are likely to be $\lesssim 10^8 \, M_\odot$ (Eddington-limited SMBH masses are typically $\sim 10^7 \, M_\odot$). The large AGN fraction in the SMG population ($\gtrsim 40\%$ for sources with $f_{850\,\mu m} \gtrsim 4$ mJy) further indicates that the SMBHs are growing almost continuously throughout these vigorous but obscured star formation episodes. The stark contrast between the AGN fractions in the SMG and coeval UV-bright galaxy populations ($\sim 3\%$; Steidel et al. 2004) suggests that this joint black hole–stellar growth activity is most strongly connected with the SMG population (Alexander et al. 2005a).

In this paper we compare estimates for the stellar and SMBH masses for a sample of 13 high-redshift protospheroids (identified with far-infrared luminous galaxies detected in the submillimeter and radio wave bands) in the northern region of the Great Observatories Origins Deep Survey (GOODS-N). These all have precise spectroscopically identified redshifts and have hard X-ray emission dominated by an AGN. The stellar mass estimates are derived from optical, near-infrared, and most importantly the mid-infrared observations of this region by the *Spitzer Space Telescope* taken as part of the GOODS survey (M. Dickinson et al. 2006, in preparation), while the SMBH mass estimates are taken from Alexander et al. (2005a, 2005b) based on the 2 Ms *Chandra* observations. Together, these data allow us to investigate the origin of the $M_\star$-M_{BH} relation for young spheroids in the early universe. Throughout, we adopt a cosmology with $H_0 = 65 \, \mathrm{km \, s^{-1} \, Mpc^{-1}}$, $\Omega_M = \frac{1}{3}$, and $\Omega_\Lambda = \frac{2}{3}$. Unless otherwise stated, masses and luminosities are given in solar units.

2. SAMPLE SELECTION AND DATA REDUCTION

For local galaxies, spatially resolved kinematics (e.g., Magorrian et al. 1998) or reverberation mapping (e.g., Wandel et al. 1999; Kaspi et al. 2000) are useful techniques for weighing the SMBHs at the center of galaxies and relating these to the stellar masses of their spheroids. However, neither of these techniques can currently be applied to SMGs at high redshifts and so by necessity we have to adopt much cruder methods to estimate both the black hole and spheroid masses. In this study we use the emission arising from accretion onto the SMBH as a tracer of the black hole mass and the rest-frame near-infrared luminosity of the galaxy as an indicator of its stellar mass.

Unfortunately, the rest-frame UV and optical spectra of the SMGs provide an ambiguous tracer of the nuclear activity in these galaxies (Chapman et al. 2005; Swinbank et al. 2004). The difficulty of merely identifying an AGN from these observations, let alone reliably estimating their luminosities, is likely caused by heavy obscuration toward the SMBH or faint broad lines from intrinsically weak AGNs being lost against the continuum of the

galaxy. Conversely, the weakness of the AGNs and their obscuration makes the use of the rest-frame near-infrared luminosity a much more reliable measure of the stellar mass of the galaxies.

In contrast, hard X-ray emission from the accretion disk emerges relatively unattenuated from all but the most obscured regions; hence the X-ray emission from SMGs may provide the most reliable probe of their SMBH masses. However, as demonstrated by Alexander et al. (2005a), only the *Chandra* 2 Ms observation of the CDF-N region (Alexander et al. 2003) reaches the necessary depth to provide constraints on the X-ray luminosities of typical SMGs. For this reason our analysis focuses on the sample of SMGs with reliable spectroscopic redshifts from Chapman et al. (2003, 2005), which lie within this field. We stress that precise redshifts are essential for our analysis. Not only are the mass estimates dependent on a well-constrained luminosity distance, but more critically there are strong degeneracies in redshift and age in the fitting of their spectral energy distributions (SEDs) described in § 3.

2.1. X-Ray Constraints on SMGs

Using the sample of spectroscopically identified, radio-detected SMGs in the CDF-N from Chapman et al. (2005), obscuration-corrected X-ray luminosities were derived for 15 galaxies and SMBH masses estimated assuming Eddington accretion by Alexander et al. (2005a, 2005b). We discard two of these galaxies from our analysis: J123716.01+620323.3 falls outside the mid-infrared coverage, and the optical/mid-infrared photometry of J123632.61+620800.1 is contaminated by a diffraction spike from a bright ($K_s \sim 14$) object only 11″ away. These conditions prevent us from estimating the stellar masses needed in § 3.2; hence we concentrate on 13 SMGs with optical, near-infrared, and mid-infrared photometry or limits and reliable spectroscopic redshifts. These galaxies range in redshift from $z = 0.5$ to 2.9, with a median comparable to that of the entire SMG population ($z = 2.2$).

The X-ray spectral analysis in Alexander et al. (2005b) shows that the bulk of the hard X-ray emission from the SMGs in our sample is likely due to accretion onto the SMBH, with star formation contributing only at the softest energies, ~ 2 keV in the rest frame. The luminosity from the X-ray wave band is only a few percent of the bolometric luminosity from the SMBH, and Alexander et al. (2005b) adopted a bolometric correction (BC$_X$) of $6^{+12}_{-4}\%$, consistent with other studies. They also employed Eddington arguments to show that $\log(M_{BH}) = \log(L_{bol}/\eta) - 38.06$, where the bolometric luminosity is in units of ergs s^{-1}. The factor η is unity for Eddington-limited accretion, and $\eta < 1$ for sub-Eddington. As our benchmark we adopt Eddington-limited accretion and use this to investigate the relation between black hole and stellar masses for our sample.

2.2. Spitzer Observations

In addition to the X-ray constraints on the luminosities and hence masses of the SMBHs, our analysis also requires estimates of the stellar masses of the host galaxies. A particularly simple and relatively robust way of deriving the mass of a stellar population is to use the rest-frame near-infrared luminosity and a theoretical mass-to-light ratio. For all but the youngest stellar populations, the rest-frame near-infrared emission is dominated by light from main-sequence stars and hence, for example, the rest-frame K-band luminosity changes by only a factor of 2 between stellar populations with ages of 100 Myr and 1 Gyr (Leitherer et al. 1999). The rest-frame V-band luminosities of the same populations, on the other hand, vary by a factor of 10. In addition to

TABLE 1
Spitzer IRAC Photometry

ID	3.6 μm	4.5 μm	5.8 μm	8.0 μm
J123636.75+621156.1............	20.51 ± 0.08	20.85 ± 0.08	21.02 ± 0.22	21.19 ± 0.14
J123721.87+621035.3............	19.25 ± 0.04	19.55 ± 0.04	19.80 ± 0.11	19.87 ± 0.05
J123629.13+621045.8............	18.96 ± 0.04	19.02 ± 0.04	19.21 ± 0.10	19.34 ± 0.06
J123555.14+620901.7............	19.81 ± 0.10	19.40 ± 0.08	19.15 ± 0.17	19.04 ± 0.09
J123711.98+621325.7............	21.46 ± 0.10	21.22 ± 0.08	20.92 ± 0.15	21.27 ± 0.08
J123635.59+621424.1............	19.35 ± 0.04	18.87 ± 0.03	18.30 ± 0.05	17.76 ± 0.02
J123549.44+621536.8[a,b]........	. . .	19.67 ± 0.30	19.45 ± 0.30	19.36 ± 0.30
J123606.72+621550.7............	21.42 ± 0.17	21.07 ± 0.11	20.69 ± 0.25	20.43 ± 0.11
J123622.65+621629.7............	20.64 ± 0.08	20.27 ± 0.05	20.03 ± 0.11	20.44 ± 0.06
J123707.21+621408.1............	20.68 ± 0.10	20.33 ± 0.08	20.02 ± 0.14	20.30 ± 0.05
J123606.85+621021.4............	20.27 ± 0.08	20.14 ± 0.06	20.03 ± 0.15	20.36 ± 0.10
J123616.15+621513.7[b]	. . .	20.65 ± 0.08	20.20 ± 0.15	19.80 ± 0.07
J123712.05+621212.3[b]	. . .	29.95 ± 0.07	20.62 ± 0.13	20.58 ± 0.05

Notes.—All magnitudes are in the AB system. Values represent total fluxes, derived by applying a correction to the measured 4″ aperture magnitudes.
[a] This sources lies on the edge of the image, although is clearly detected. In these cases we set the error to 0.3 mag to reflect the uncertainty in our aperture fluxes.
[b] The 3.6 μm images for these sources were confused, and SExtractor could not converge on a solution. Since the other photometry is sufficient to constrain the shape of the SED, we choose not to use the data from this band.

its relative insensitivity to age variations, the rest-frame K band is over 10 times less sensitive to reddening than V band, which is important to consider for these dusty SMGs.

At the redshift of our targets, the rest-frame K band is shifted toward the mid-infrared and hence *Spitzer* observations are required to estimate the stellar mass. For this reason, we obtained the IRAC images of GOODS-N from the *Spitzer* archive (V.1 20041027 and V.1 20050505 enhanced data products). We used SExtractor (Bertin & Arnouts 1996) to measure the photometry and uncertainties in these for each of the galaxies on the IRAC imaging. By constructing curves of growth for several isolated objects, we determined that 9″ diameter apertures were necessary to measure the total IRAC flux from our targets. Since source confusion is an issue for these extremely deep exposures, we used 4″ diameter apertures and then applied a small aperture correction, determined to be 0.32, 0.37, 0.49, and 0.55 mag for the 3.6, 4.5, 5.8, and 8.0 μm bands, respectively. Even so, we were unable to adequately constrain the 3.6 μm flux for three sources due to confusion noise from nearby sources. We provide the IRAC

photometry for all 13 sources in Table 1. At 5.8 μm, which corresponds to a rest-frame wavelength of ~2 μm, the 10 high-redshift SMGs at $z > 1.8$ have a bright mean magnitude of 20.1 ± 0.8, with the entire sample spanning under an order of magnitude in flux. This is in contrast with the R-band fluxes, which cover well over an order of magnitude. The modest dispersion in the mid-infrared fluxes of the SMGs already suggests that we are dealing with a relatively homogeneous population of luminous, high-redshift galaxies.

2.3. *Spectral Energy Distributions*

To improve the constraints on the form of the SEDs in SMGs, we also make use of rest-frame UV/optical photometry to extend the wavelength coverage and so estimate the likely reddening and ages of the stellar populations. For this we use the $UBVIRz'$ photometry presented in Capak et al. (2004). These data were supplemented with J- and K_s-band near-infrared imaging from the WIRC2 camera at Palomar (see Bundy et al. 2005 and Smail et al. 2004 for a description of these data). Combined, these

TABLE 2
Ground-based Optical and Near-Infrared Photometry

ID	U	B	V	R	I	z'	J	K_s[a]
J123636.75+621156.1.....	24.28 ± 0.08	23.43 ± 0.05	23.09 ± 0.03	22.39 ± 0.02	21.84 ± 0.02	21.61 ± 0.03	21.12 ± 0.04	20.58 ± 0.04
J123721.87+621035.3.....	24.19 ± 0.08	24.00 ± 0.07	23.52 ± 0.04	22.81 ± 0.02	21.84 ± 0.03	21.35 ± 0.02	. . .	19.84 ± 0.02
J123629.13+621045.8.....	26.11 ± 0.25	25.70 ± 0.15	24.98 ± 0.09	24.05 ± 0.04	22.89 ± 0.04	22.36 ± 0.04	21.39 ± 0.05	19.93 ± 0.02
J123555.14+620901.7.....	24.38 ± 0.09	24.24 ± 0.08	24.16 ± 0.05	23.80 ± 0.04	23.45 ± 0.06	23.16 ± 0.06	21.99 ± 0.09	20.92 ± 0.05
J123711.98+621325.7.....	26.12 ± 0.26	25.75 ± 0.14	25.71 ± 0.16	25.66 ± 0.13	24.99 ± 0.18	25.06 ± 0.24	>24.0	>23.1
J123635.59+621424.1.....	23.94 ± 0.07	24.06 ± 0.07	24.00 ± 0.05	23.79 ± 0.04	23.36 ± 0.06	23.11 ± 0.06	21.99 ± 0.09	20.74 ± 0.04
J123549.44+621536.8.....	24.61 ± 0.10	23.93 ± 0.07	23.60 ± 0.04	23.27 ± 0.03	23.01 ± 0.04	22.84 ± 0.05	21.77 ± 0.07	21.49 ± 0.18[a]
J123606.72+621550.7.....	23.75 ± 0.06	23.32 ± 0.06	23.29 ± 0.03	23.26 ± 0.03	23.09 ± 0.05	23.06 ± 0.06	>24.0	>22.8[a]
J123622.65+621629.7.....	25.62 ± 0.17	25.17 ± 0.14	25.09 ± 0.11	24.85 ± 0.08	24.45 ± 0.13	24.21 ± 0.14	>24.0	22.25 ± 0.15
J123707.21+621408.1.....	>27.8	26.77 ± 0.27	26.36 ± 0.29	25.63 ± 0.14	25.51 ± 0.30	24.69 ± 0.19	>24.0	21.86 ± 0.11
J123606.85+621021.4.....	26.17 ± 0.26	25.25 ± 0.14	25.15 ± 0.10	24.41 ± 0.06	24.21 ± 0.10	23.93 ± 0.10	22.20 ± 0.10	20.98 ± 0.05
J123616.15+621513.7.....	>27.8	26.59 ± 0.24	26.13 ± 0.22	25.36 ± 0.11	25.03 ± 0.18	25.00 ± 0.23	>24.0	22.71 ± 0.23
J123712.05+621212.3.....	>27.8	>27.6	>27.6	>27.4	>26.4	>26.2	>24.0	23.02 ± 0.30

Notes.—All magnitudes are in the AB system. For undetected sources, we quote 2.5 σ upper limits. The J and K_s magnitudes are measured in 4″ apertures, while all other bands use 3″.
[a] Two sources that fall outside our K_s coverage are in the HK' catalog provided by Capak et al. (2004), so we use those values here.
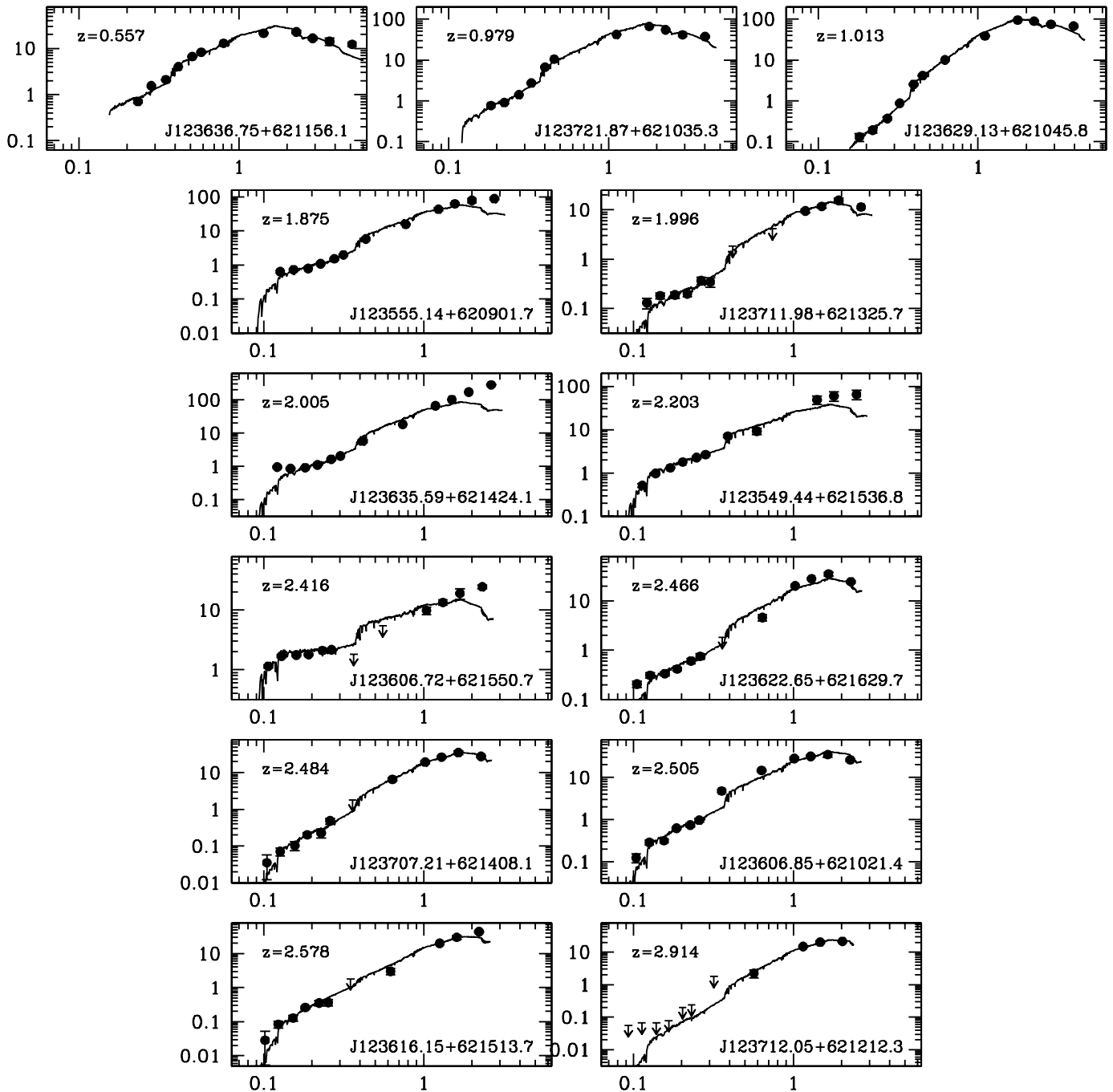
Fig. 1.—SEDs of the 13 SMGs with black hole mass estimates from Alexander et al. (2005b), ordered in increasing redshift. The top line shows the SEDs of the lower redshift SMGs, while the remaining 10 are all at $z > 1.8$. The best-fit template from Hyper-z is overlaid on the measured photometry (in units of μJy), and the wavelengths (shown in units of μm) are corrected to the rest frame at the redshift noted. [*See the electronic edition of the Journal for a color version of this figure.*]

ground-based data cover more bands than the GOODS-N *Hubble Space Telescope* (*HST*) ACS imaging of this field (Giavalisco et al. 2004). Although the extra bands provided by the ground-based imaging are essential for the SED template fitting (see § 3.1), the high-resolution imaging available from *HST* is valuable for studying the light profiles of these galaxies. C. Borys et al. (2006, in preparation) show that the rest-frame *V*-band light distributions of a sample of 27 SMGs (5 of which are in the sample presented here) follow an $r^{1/4}$ power law on average, consistent with the spheroidal nature of these systems. A summary of the optical and near-infrared photometry is presented in Table 2. We adopt 3″ and 4″ diameter apertures to measure the fluxes from the optical

and near-infrared imaging as these provide optimal signal-to-noise ratios and a near-total estimate of the magnitudes for the SMGs.

We plot the combined optical, near-, and mid-infrared photometry for the 13 SMGs in Figure 1. The SEDs for these galaxies show three clear features: a sharp decline at rest-frame wavelength of $\leq$912 Å resulting from the Lyα limit within the galaxy and the foreground intergalactic medium, a break at around 4000 Å arising either from the spectral breaks found in young or evolved stellar populations at this approximate wavelength, and finally a peak in the emission at $\sim$1.6 μm associated with the minimum in the H$^-$ opacity (John 1988; Simpson & Eisenhardt 1999) and hence the maximum emission from stellar atmospheres.

Looking at the SEDs in Figure 1 we conclude that there is a modest range in the rest-frame UV/optical/near-infrared properties of radio-detected SMGs. However, focusing on the 10 higher redshift SMGs, at $z > 1.8$, of those with full coverage of their rest-frame UV and optical SEDs, 80% show a detectable discontinuity in their SEDs around 4000 Å in the rest frame (Fig. 1). We interpret this break as arising from the Balmer limit in stellar populations with ages of hundreds of Myr. This interpretation is consistent with the likely nature of SMGs as luminous far-infrared sources seen during a phase of intense star formation. We note that age-related differential reddening may also account for the relative strength of this feature in an even younger ongoing starburst (Poggianti & Wu 2000).

3. ANALYSIS AND RESULTS

3.1. *Estimating Stellar Masses*

Due to the complex mix of extinction expected within SMGs (Chapman et al. 2004), which may influence different age stellar populations to different degrees, we have adopted a very simple approach in determining our stellar masses. We first estimate the rest-frame K-band luminosities of the galaxies, interpolated if necessary from a fit to the SED, and then combine these with estimates of the mass-to-light ratios in the K band for a range of plausible ages for the dominant stellar population.

To derive the rest-frame K-band luminosities we exploit the Hyper-z package (Bolzonella et al. 2000) to fit physically meaningful spectral templates to the SEDs of each galaxy and then estimate their K-band luminosities by interpolation of the best-fit templates. This approach has the added advantage that the properties of the best-fit spectral templates may provide some insights into the properties of the stellar populations within these galaxies. We restrict the code to fit the SEDs at the spectroscopically confirmed redshift, and allow it to choose between two model SED templates: one having an instantaneous burst of star formation, or one with a constant star formation (CSF) history. These represent the two extremes of the likely star formation histories for these young galaxies (Smail et al. 2003) and provide an adequate variety to guarantee a reliable estimate of the K-band luminosity for those galaxies whose SEDs are dominated by starlight. In our fits, the reddening (A_V) was free to vary and the ages at the galaxy's redshift were constrained to be physical within our adopted cosmology. These provide additional degrees of freedom for the fitting and may give some indication of the properties of the composite stellar population in these systems.

For each galaxy, Hyper-z returns the absolute magnitude in the rest-frame K band, as well as the age, reddening, and star formation history of the best-fit template. Although the M_K values are not corrected for it, the reddening (which is $\sim 0.1 A_V$ based on the extinction law presented in Calzetti et al. 2000) has a negligible effect on our stellar mass estimates, particularly compared with other uncertainties in our analysis. The typical fit to a SED in our sample produces a reasonable χ^2, with only three minor exceptions: Both J123635.59+621424.1 and J123606.72+621550.7 are spectroscopically identified AGNs and demonstrate an obvious excess at the reddest wavelengths. This would be expected, since the input templates do not account for the contribution in the mid-infrared of warm dust from an AGN. J123549.44+621536.8 also has a moderate near-infrared excess, but the significance is muted somewhat by its proximity to the edge of the IRAC map, where photometry was more difficult to estimate. The starburst J123606.85+621021.4 has an excess in the UV, but this is caused by a contribution from an unrelated blue foreground ($z = 0.4$) galaxy only $2''$ away. In all these cases, we feel the

best-fit SED template is still a good measure of the rest-frame K-band luminosity and provides a good estimate of the underlying stellar mass. As we show below, changes to the implied stellar masses of factors of 2 (due to AGN contamination at rest-frame K band) would not significantly alter the conclusions of this work.

To convert these estimates for M_K into stellar masses, we need to determine the light-to-mass ratio, L_K/M, for the dominant stellar populations in these galaxies. To do this we turn to the Starburst99 stellar population model (Leitherer et al. 1999), which provides estimates of M_K for our two extreme scenarios, either a burst or CSF history. We adopt the initial mass function (IMF) of Miller & Scalo (1979); this is also the same as that used for the Hyper-z templates. The IMF has a mass range of $0.1–125\,M_\odot$ and assumes solar metallicity. Higher metallicities are often favored when fitting the SEDs of ultraluminous infrared galaxies (ULIRGs) in the local universe (e.g., Farrah et al. 2005), but we found no appreciable difference in the estimates of L_K/M for a range of likely values.

We can combine the predicted K-band luminosities as a function of time from Starburst99 with the integrated stellar masses at that time to derive the effective light-to-mass ratio for the stellar population:

$$L_K/M = 10^{-0.4(M_K - 3.3)}/\Sigma[M_*(t)], \qquad (1)$$

where 3.3 is the absolute magnitude of the Sun in the K band (Cox 2000). We find that the light-to-mass ratio for the CSF case is reasonably described by a simple power law, $L_K/M = 103(\tau/\text{Myr})^{-0.48}$ for $\tau > 100$ Myr. The behavior of L_K/M for a burst model is not as easy to parameterize over the likely range of ages of SMGs, so instead we use tabulated values. In solar units, we find that L_K/M is 2.5, 2.2, 13.3, 7.6, 4.2, 2.7, and 1.9 at 10, 20, 50, 100, 200, 500, and 1000 Myr, respectively. We caution the reader that at ages of <50 Myr changes to the adopted IMF or metallicity can have significant effects on the L_K/M and so the predictions for extremely young bursts are much more uncertain.

In principle, we can constrain the ages of the dominant stellar population in each SMG from our SED modeling. However, the correlated nature of the fits and the fact that we are likely sampling different mixes of stellar populations at different wavelengths due to differential reddening mean that the results are highly uncertain for individual galaxies. To demonstrate this point, we note that all of the galaxies can be reasonably fit by *either* model star formation history, but with very different ages. This is a direct consequence of the fact that an older galaxy with a CSF history has a similar SED to that of a younger burst model, a point also noted in Shapley et al. (2001, 2005). For this reason we prefer to use only ensemble averages for the derived parameters. If we restrict our Hyper-z fits to the burst model only, we estimate ensemble averages of 250 ± 190 Myr, $A_V = 1.7 \pm 0.2$, and $M_K = -26.3 \pm 0.3$. Alternatively, restricting our fits to just the continuous star formation model yields 2000 ± 500 Myr, $A_V = 1.7 \pm 0.3$, and $M_K = -26.4 \pm 0.3$.

For the average age from our fits of the burst model, we estimate a typical $L_K/M = 3.7$, while the average for the continuous star formation model is $L_K/M = 2.6$. Hence, the average stellar mass from the samples, estimated using M_K and L_K/M, are essentially identical, $\log(M_{\text{burst}}) = 11.3 \pm 0.4$ and $\log(M_{\text{CSF}}) = 11.5 \pm 0.4$. Based on these results, we choose to simply use $L_K/M = 3.2$ for all galaxies. Given the degeneracy between the SED fits, we use the average M_K from the burst and CSF fit for each galaxy, and half the difference between them as a measure

TABLE 3
Derived Optical and X-Ray Parameters for a Sample of SMGs in GOODS-N

ID	z[a]	M_K[b]	$\log(M_\star)$[c]	$\log(L_X)$[d]	$\log(M_{BH})$[d]	Fit Quality[e]
J123636.75+621156.1	0.557	-24.13 ± 0.03	10.56 ± 0.02	42.7	$6.0^{+0.3}_{-6.0}$	
J123721.87+621035.3	0.979	-26.22 ± 0.04	11.39 ± 0.01	43.7	$6.8^{+0.5}_{-0.5}$	
J123629.13+621045.8	1.013	-26.42 ± 0.03	11.47 ± 0.02	43.2	$6.3^{+0.5}_{-0.3}$	
J123555.14+620901.7	1.875	-27.30 ± 0.22	11.82 ± 0.15	44.4	$7.6^{+0.5}_{-0.5}$	
J123711.98+621325.7	1.996	-25.58 ± 0.22	11.14 ± 0.16	43.6	$6.8^{+0.5}_{-0.5}$	
J123635.59+621424.1[f]	2.005	-28.12 ± 0.24	12.15 ± 0.20	44.0	$7.1^{+0.5}_{-0.4}$	Near-IR excess
J123549.44+621536.8[f]	2.203	-27.91 ± 0.22	12.07 ± 0.13	44.0	$7.1^{+0.5}_{-0.5}$	Near-IR excess
J123606.72+621550.7	2.416	-27.41 ± 0.26	11.87 ± 0.12	43.8	$7.0^{+0.5}_{-0.4}$	Near-IR excess
J123622.65+621629.7[f]	2.466	-26.52 ± 0.30	11.51 ± 0.23	44.0	$7.2^{+0.5}_{-0.5}$	
J123707.21+621408.1[f]	2.484	-26.52 ± 0.02	11.51 ± 0.08	43.8	$6.9^{+0.5}_{-0.4}$	
J123606.85+621021.4[f]	2.505	-27.12 ± 0.32	11.75 ± 0.15	43.7	$6.8^{+0.5}_{-0.5}$	UV excess
J123616.15+621513.7	2.578	-26.50 ± 0.09	11.50 ± 0.05	43.7	$6.8^{+0.5}_{-0.5}$	
J123712.05+621212.3	2.914	-25.84 ± 0.01	11.24 ± 0.06	43.4	$6.6^{+0.5}_{-0.6}$	

[a] Redshift determined from UV spectroscopy (Chapman et al. 2005).
[b] Absolute K-band magnitude derived from Hyper-z (uncorrected for reddening).
[c] Stellar mass in units of $M_\odot$ derived assuming $L_K/M = 3.2$.
[d] Rest-frame 0.5–8.0 keV luminosity (in units of ergs s^{-1}) and SMBH mass in units of $M_\odot$ from Alexander et al. (2005a) assuming a bolometric correction of 6%, with an uncertainty reflecting the possible range in this correction.
[e] SED fit was deemed good unless otherwise notes. See § 3.1.
[f] These five SMGs also have rest-frame optical spectroscopy from Swinbank et al. (2004).

of the uncertainty. We summarize the results of our stellar mass estimates from the SED fitting in Table 3. The mean stellar mass is $\log(M_\star) = 11.4 \pm 0.4$ for the sample of SMGs used here.

3.2. The $M_\star$-M_{BH} Relation

Figure 2 shows the rest-frame V-band and K-band luminosities from our SED fits against the X-ray luminosities from Alexander et al. (2005b). There is an apparent trend between K-band and X-ray luminosity, which is reasonably fit by a power law of the form $L_K \propto L_X^{0.64 \pm 0.06}$. To test the strength of the correlation, we applied a Spearman rank test, The correlation coefficient is 0.68, with a $2.4\,\sigma$ deviation from the null hypothesis that L_K and L_X are not correlated. Removing the three lower redshift sources in Figure 2 does weaken the apparent correlation: the power-law index becomes 0.79 ± 0.32, while the Spearman test estimates a $1.8\,\sigma$ deviation from the null hypothesis. While the modest dynamic range of our sample makes evidence for a correlation difficult to find, as we discuss below, it does yield strong constraints on the normalization of the relationship.

For both the full sample and with the three lower redshift sources excluded, the trends with K-band magnitude are 3 times tighter than that seen between the reddening-corrected rest-frame V-band magnitude and X-ray luminosities, yielding an rms of 0.6 and 2.0 mag, respectively. This difference most likely reflects the increased sensitivity to reddening corrections in the rest-frame V band, in addition to the fact that near-infrared luminosities better probe the evolved stellar population. Since the uncertainty in the stellar mass estimates scale as $0.4\Delta_{mag}$ dex, these results underline the advantages of the rest-frame K-band luminosities to estimate the stellar masses of these galaxies.

If we assume that the X-ray emission arises from accretion onto SMBHs, as indicated by the spectral analysis of Alexander et al. (2005b), we can interpret the correlation between L_K and L_X as one between the stellar component of the galaxies and their SMBHs. Such a correlation would also be expected if the K-band light were due to hot dust powered by the AGN. However, with only a few exceptions, the SEDs seem to be dominated by stellar light, as evident from a well-defined stellar bump peaking near 1.6 μm (Fig. 1). For the remainder of the paper we assume that

the K band is tracing the stellar mass, but the reader should bear the caveat in mind.

In Figure 3 we plot the distribution of $M_\star$ (the stellar mass from the SED fits assuming a fixed L_K/M) and $M_{BH,Edd}$ (the SMBH masses derived from the absorption-corrected X-ray luminosities
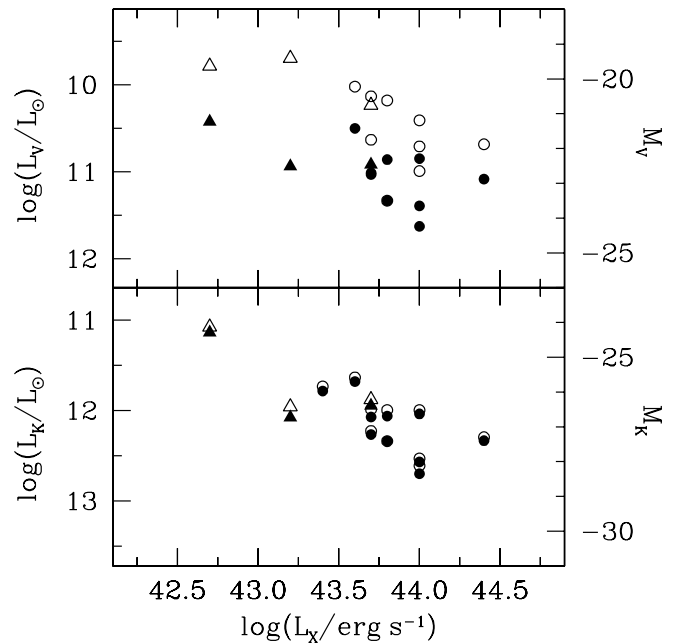

Fig. 2.—We show the correlation between the rest-frame V- and K-band luminosities and the rest-frame absorption-corrected 2–10 keV luminosities of the 13 high-redshift SMGs in our sample. Open symbols represent the optical luminosities uncorrected for reddening. The best-fit values of A_V from Hyper-z were used to correct these values for reddening, and we show them as the filled points. Circles represent the 10 $z > 1.8$ subsample, while triangles are the three lower redshift sources. The K-band panel shows a clear trend for more luminous galaxies to have higher X-ray luminosities, as expected if they host more massive black holes. A similar trend may be seen in the V-band panel; however, this is masked by the increased sensitivity to the reddening correction and the corresponding uncertainties. In order to keep the scales the same between the two panels, we excluded J123712.05+621212.3 from the V-band plot, since it falls considerably outside the range (with $M_V = -13.5$).
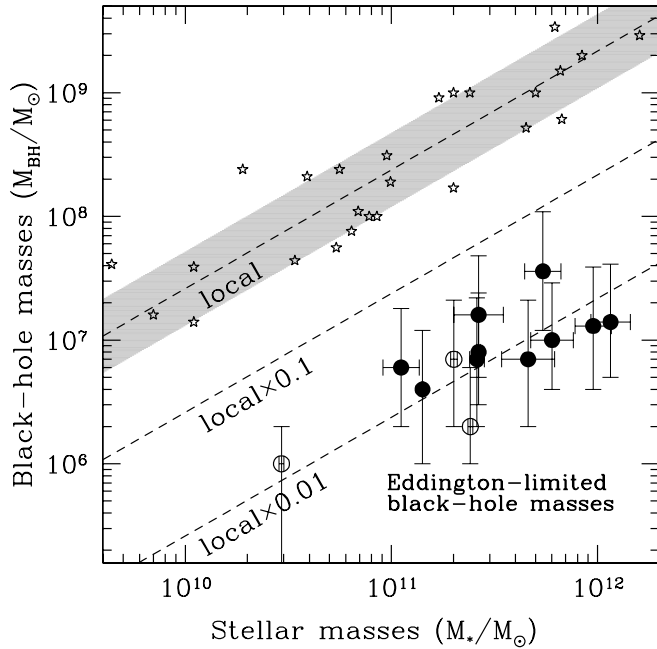
Fig. 3.—Relationship between stellar and SMBH masses for our sample of 13 high-redshift SMGs. Black hole masses are derived using the assumption of Eddington-limited accretion (see § 3.2). Stellar masses are derived by using the rest-frame K-band absolute magnitude derived from the fits to the SEDs in Fig. 1 and assuming $L_K/M = 3.2$ for all galaxies. The upper dashed line denotes the best fit to local galaxies (shown as stars) as derived by Marconi & Hunt (2003), and the gray area denotes the region where 68% of the local points are contained. The lower dashed lines denote tracks with black hole masses 1/10 and 1/100 of the local relation. The three SMGs shown as open symbols are those lying at redshifts of $z < 1.8$. [See the electronic edition of the Journal for a color version of this figure.]

by Alexander et al. [2005a] assuming Eddington accretion and a $6^{+12}_{-4}\%$ bolometric correction). As in Figure 2, we see a reasonable correlation between these two quantities.

The limited dynamic range of our sample and the uncertainties in the individual measurements means we cannot provide a reliable constraint on the power-law index for this correlation, $M_{BH} \propto M_\star^\gamma$. The data are consistent with $\gamma \sim 0.3-1$, with a very large uncertainty depending upon the exact choice of sample used. Nevertheless, while the slope of the correlation is uncertain, the normalization is well constrained at the mean $M_\star$ of our sample. At $\log(M_\star) = 11.4 \pm 0.4$, we find that the average Eddington-limited black hole mass is $\log(M_{BH,Edd}) = 6.86 \pm 0.40$. If we exclude the three SMGs at $z < 1.8$, the mean stellar and black hole masses are slightly larger: $\log(M_\star) = 11.5 \pm 0.32$ and $\log(M_{BH,Edd}) = 7.00 \pm 0.27$.

As a comparison we turn to a sample of nearby (<250 Mpc) galaxies with reliable black hole masses estimated from high-resolution HST spectroscopy and stellar masses derived via near-infrared observations of the host galaxies (Marconi & Hunt 2003). Although their full sample includes 37 galaxies, we concentrate on the 27 "group 1" systems judged by those authors to be the most secure. Using these data, Marconi & Hunt (2003) showed that

$$\log(M_{BH}) = (8.28 \pm 0.06) + (0.96 \pm 0.07) \log\left(\frac{M_{bulge}}{10^{10.9}}\right). \quad (2)$$

We note that this relation predicts black hole masses roughly 50% higher than those presented in Häring & Rix (2004), who used Jeans equation modeling rather than virial estimators to predict the bulge mass.

Using these relations, our data suggest that the black hole masses we infer for SMGs (either in the full sample or for the 10 SMGs at $z > 1.8$) are ~ 50 times smaller than for similarly massive local spheroids.

4. DISCUSSION

With the assumptions about the L_K/M and Eddington fraction η that we have adopted, our results suggest that the black holes in SMGs require significant growth in order to approach the present-day relation. To understand the significance of this conclusion, however, we need to better characterize any biases in the mass estimates for both of these components. Note that errors on individual sources are large in principle, since for both the black hole and stellar masses we have assumed ensemble values (i.e., fixed η for the black holes and a single L_K/M value for all stellar mass estimates). It is quite likely that source-to-source variations will affect the scatter of the data, but until more accurate methods are available for the mass estimates, we concentrate instead on understanding any systematic bias that could affect the sample as a whole.

Altogether, the ratio between our black hole masses and those in the nearby universe scales as

$$50\left(\frac{\eta}{1.0}\right)\left(\frac{3.2}{L_K/M}\right)\left(\frac{BC_X}{0.06}\right), \quad (3)$$

where we have simplified the expression by assuming the power-law relation between stellar mass and black hole has an exponent of 1.0. In Figure 4 we plot tracks of different conditions where the above expression is unity. This demonstrates how difficult it is for any one factor to explain the difference between our sample and the local relation, and suggests either that the discrepancy is real or that biases in the parameters must conspire if, in fact, SMGs have a black hole/stellar mass ratio comparable to local systems. We now discuss these potential biases in more detail.

4.1. Factors Influencing Stellar Mass Estimates

We begin by pointing out that the stellar masses that we derived are on average 5 times higher than those reported from modeling the UV/optical SEDs of SMGs in Smail et al. (2004). This contrasts with the reasonable agreement in the estimated stellar masses derived for UV-selected galaxies at redshifts similar to those of the SMGs by Shapley et al. (2005) from both rest-frame UV/optical and rest-frame UV/optical/near-infrared photometry. We attribute the difference in our masses from those from Smail et al. (2004) to the absence of mid-infrared information to constrain the SED modeling in the earlier work, which is thus much more sensitive to the reddening corrections derived from the SED fits to these very dusty galaxies and the possibilities of strong differential reddening within their young stellar populations.

In our modeling of the stellar mass of the systems we adopted an L_K/M ratio of 3.2, characteristic of a burst with an age of ~ 250 Myr. If we require that the SMG and the present-day $M_\star$-M_{BH} relations agree, then from equation (3) we see that the stellar masses must drop by a factor of ~ 50. This corresponds to $L_K/M \sim 250$, which is not possible with the Miller-Scalo IMF. For a Salpeter IMF, such a high L_K/M ratio implies ages for the SMGs of $\lesssim 10$ Myr. We discuss the implications of varying the IMF later in this section.

However, we note that there are fundamental inconsistencies in our calculations if we rigidly interpret the star formation histories we used. The SMGs in our sample have been selected on the basis of their intense far-infrared luminosities, which implies high
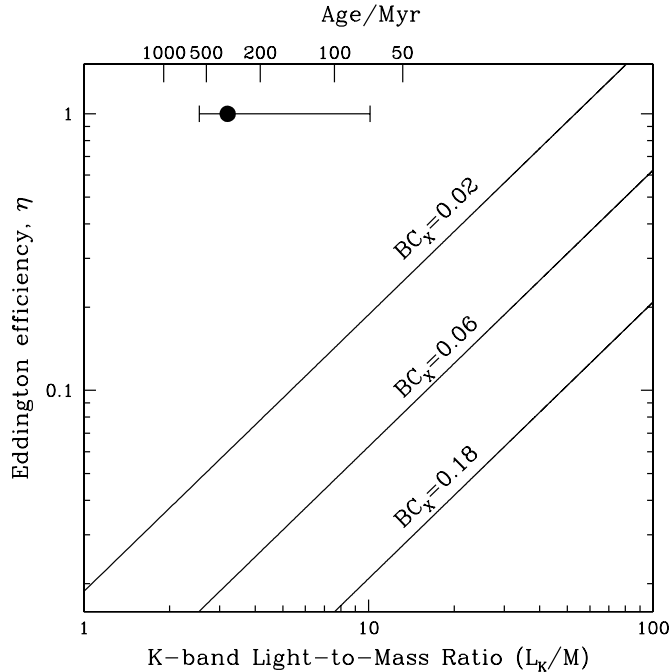
FIG. 4.—This figure graphically illustrates the available parameter space required to place the SMBH and stellar masses of the high-redshift SMG sample onto the local $M_\star$-M_{BH} relation. The solid lines represent combinations of L_K/M and η that would bring our mass estimates in line with the local relation at a given assumed value for the X-ray bolometric correction. They span the estimate for BC_X determined by Elvis et al. (1994). We plot our best estimate for the values of L_K/M and η as the filled circle. As an example to help illustrate the use of this figure, assume a 6% X-ray to bolometric luminosity correction and an Eddington efficiency of 0.1; the plot then indicates that our stellar ages need to be ~50 Myr in order to make the data agree with the local relationship. The plot does not account for a possible missing fraction of X-ray flux due to heavy obscuration in the SMGs. This would systematically push the black hole mass estimates up, and the three lines closer to our observed point. See § 4.2 and Alexander et al. (2005b) for more details.

star formation rates. The fast decline in the far-infrared emission from a starburst after star formation ceases (Kennicutt 1998) indicates that star formation is currently ongoing in these systems or has declined significantly in only the last few tens of Myr. The submillimeter detection of these sources is therefore formally inconsistent with the star formation history in our burst model, where there has been no star formation within the galaxy in the past ~250 Myr. Although the alternative CSF models include ongoing star formation, the much higher ages derived from these fits are equally inconsistent with a constant rate of star formation at the level indicated by the observed far-infrared emission from the SMGs, ~$(1-2) \times 10^3 \ M_\odot \ yr^{-1}$ (Kennicutt 1998). To form an $M_K \sim -26.4$ galaxy with a constant SFR at this level would take just ~100 Myr, not the 2 Gyr derived from the fits.

There are two solutions to solve these inconsistencies within our models: (1) allow a more complex star formation history, most likely involving a recent burst of activity; (2) apply age-dependent dust extinction to the stellar populations, with the youngest stars being most extincted. As both solutions involve additional free parameters to what is already a weakly constrained problem, we will only qualitatively discuss their impact.

Bursts of star formation are a natural consequence of interaction-induced activity due to the cyclic behavior of bound orbits (Mihos & Hernquist 1994). They lead to a dispersion in the properties of SMGs dependent on the number of previous bursts they have experienced. The main consequence in terms of our analysis is the realization that the present activity may not have produced the total stellar population that we observe. Mixing in a fraction of older stars will systematically decrease the effective L_K/M, potentially increasing the masses of the galaxies. This would therefore push the SMGs even further away from the $z = 0 \ M_\star$-M_{BH} relation.

Age-dependent or selective extinction of the stellar populations (e.g., Poggianti et al. 2001) within SMGs can preferentially extinguish the UV emission from the youngest stars. This results in SEDs with much redder spectral indices between the UV and near-infrared than can be achieved with a simple foreground dust screen acting upon the whole stellar population. When the diffusion timescale for stars to escape their obscured birthplaces is around a few hundred Myr, this process can also help reproduce the strength of the spectral breaks at ~4000 Å, even in galaxies with significant ongoing star formation. As a result, selective extinction would provide the opportunity to fit the SED of our SMG sample with relatively young CSF models, ~100 Myr, consistent with the ages needed to produce their observed near-infrared luminosities given the star formation rates inferred from their far-infrared emission.

Attempts to estimate typical ages for SMGs include the spectral dating of the few examples with high-quality UV spectroscopy. Such an analysis by Smail et al. (2003) indicates an age for a UV-bright SMG of ≳10 Myr, similar to the minimum age that we require. However, as Smail et al. (2003) state the SMG they model may be a rare system, and the small proportion of SMGs showing similar signs of young stellar populations in their spectra suggests that a more typical age for an SMG would be 50–100 Myr. Another estimate of the likely age of SMGs can be derived via gas-depletion timescales using the measured mass of the gas reservoir, and the estimated star formation rates suggest likely lifetimes of ≳30 Myr (Greve et al. 2005), where we have assumed an AGN contribution to the far-infrared luminosities in line with Alexander et al. (2005b). Finally, taking our estimated stellar masses and the median star formation rates derived from the far-infrared luminosities of the SMGs in our sample using our adopted IMF, we determine lifetimes of ~100 Myr to produce the stellar populations we see. Balancing these estimates with those from the SED fitting, we conclude that the typical ages of SMGs are likely to be ≳50 Myr. Hence the stellar masses are inconsistent with what would be predicted from the local $M_\star$-M_{BH} relation assuming that our black hole masses are accurate.

Are there other ways to change the effective L_K/M without invoking such young ages? One way to reduce it is to have a significant contribution to the rest-frame K-band light from the AGN. However, the bulk of our sample, as evident in Figure 1, are well fit by a stellar component only. In the few cases where AGNs cause the SED fits to diverge at the longer wavelengths, the estimated luminosity that we derive at 2.2 μm is still dominated by the stars. We used the 8 μm excess (the ratio of the measured 8 μm flux over that derived from the best-fit model template) to quantify possible AGN contamination. We find that the $z > 1.8$ sources (excluding the 3 marked as having an obvious near-infrared excess) have an average excess of 1.0, suggesting little or no contribution from an AGN. The remaining three sources, however, have an average excess of 2.3, which means a nearly equal contribution to the rest-frame K-band from AGNs as from stars. Scaling down the stellar masses of these three galaxies to account for this results in only a ~0.1 reduction in the mean stellar mass of the sample, which is small considering the other factors we discuss.

In addition to contribution of light from the AGNs, we note that our analysis includes light from *all* of the stars, not simply from the bulge component used in deriving the local relation.

While the high-resolution *HST* NICMOS imaging verifies that the rest-frame *V*-band light in SMGs is reasonably fit by an $r^{1/4}$ surface brightness profile (C. Borys et al. 2006, in preparation), some systems do show a significant disk component. Whether these stars are still in a disk component at the present day or whether they would have been driven into the bulge through, for example, bar instabilities is impossible to verify, and so we flag this to the reader as a fundamental uncertainty of our analysis. Nevertheless, we note that any correction to the stellar masses due to a disk component is unlikely to change the inferred spheroid mass by more than a factor of 2–3 for a small fraction of the SMGs.

The IMF also has a significant effect on stellar mass estimates. Baugh et al. (2005) argue that an IMF biased to more massive stars is required to reproduce the properties of SMGs in current semianalytic galaxy formation models, and they invoke a power-law IMF with an index flatter than the canonical Salpeter (Salpeter 1955) slope of $\alpha \sim 2.35$. We used Starburst99 to study the effect of this top-heavy IMF on our mass estimates, but find that the stellar mass estimates change by at most a factor of ~ 3 for the range of likely ages for SMGs. An additional factor of 3 in the light-to-mass ratio can be picked up by truncating the IMF at $\sim 1\ M_\odot$, and there are different IMF prescriptions (such as the one proposed by Maraston et al. [2005] that has an increased *K*-band contribution from thermally pulsating AGB stars) that can also increase the effective light-to-mass ratio. Altogether, it is possible that these effects could conspire to decrease our stellar masses by up to a factor of ~ 10. However, we conclude that any bias present in the stellar mass is insufficient by itself to account for the difference between our results and the local relation.

4.1.1. *Tests of the Stellar Masses*

Are the high stellar masses that we derive in conflict with other estimates of the masses of SMGs?

Dynamical masses for SMGs from CO spectroscopy with millimeter interferometers indicate a median gas+stellar mass of $\log(M_{\rm dyn}) \sim 11.1 \pm 0.3$ within the central $\lesssim 10$ kpc of typical SMGs with 850 μm fluxes of a few mJy (Frayer et al. 1998, 1999; Neri et al. 2003; Greve et al. 2005). In addition, five of the galaxies in our sample have dynamical mass estimates from Hα spectroscopy (Swinbank et al. 2004), which all give constraints on the masses of $\log(M_{\rm dyn}) \sim 11.0$–11.3, again on ~ 10 kpc scales. In a recent analysis, Greve et al. (2005) use the integrated CO line luminosities for 12 SMGs to estimate an average contribution from gas of $\log(M_{\rm gas}) = 10.5 \pm 0.2$ within $\lesssim 10$ kpc for these systems. Thus taking into account the contribution from gas, the dynamical estimates are consistent with the presence of $\log(M_*) \sim 11$ of stars within the central regions of the SMGs.

As highlighted by Swinbank et al. (2004), the Hα dynamical mass estimates derived from the Hα line widths for SMGs are 5 times higher than similar constraints on UV-selected galaxies at comparable redshifts (Erb et al. 2003). To see if this difference is also reflected in the stellar mass estimates for the two populations, we ran our Hyper-z analysis on the sample of 72 spectroscopically confirmed, UV-selected, and IRAC-detected galaxies at $z \sim 2.3$ presented in Shapley et al. (2005). These UV-selected galaxies (Adelberger et al. 2004; Steidel et al. 2003) make an ideal comparison set, as they are more modestly star-forming galaxies at roughly the median redshift of our sample. As with our analysis, the fits to the data from Shapley et al. (2005) were degenerate in SED template, age, and reddening. Roughly one-third of the objects are best fit by a young (~ 50 Myr) burst while the remainder are better modeled by a CSF history with an age of ~ 600 Myr. Again we find that the choice of model has little impact on the derivation of the stellar mass, and we obtain a mean

of $\log(M_*) = 10.35 \pm 0.34$ for this sample. The estimated ages and masses are in good agreement with the results which Shapley et al. (2005) derive using a more detailed analysis [$\log(M_*) = 10.32 \pm 0.51$]. This confirms that our approach to stellar mass estimation is robust and also suggests that the SMGs in our sample are on average ~ 10 times more massive than the UV-selected population at $z \sim 2.2$.

Overall, we conclude that our stellar masses are consistent with dynamical limits on the masses of the SMG population and support the suggestion that the central regions of these galaxies are baryon dominated. We note that the CO detections of SMGs indicate that there is sufficient gas present to continue to build the black hole, but at the same time the gas masses are small enough that they will not appreciably change the stellar masses even if the bulk of it is converted into stars. Only by bringing in more gas or stars into these systems (through cooling or mergers) can their stellar masses be significantly increased from what we measure.

4.2. *Factors Influencing Black Hole Mass Estimates*

Is it possible that the sources only appear to lie below the local relation because the black hole mass estimates from Alexander et al. (2005a) are too low? Certainly, in the light of the discussion above it appears that the black hole mass estimates are probably the more important source of uncertainty in our analysis. In estimating the black hole masses, Alexander et al. (2005a) assumed Eddington-limited accretion and a $6^{+12}_{-4}\%$ bolometric correction to convert the observed absorption-corrected L_X to $M_{\rm BH,Edd}$. Since the Eddington limit appears to provide a reasonable upper bound to the accretion rate of black holes (e.g., McLure & Dunlop 2004), this approach essentially provides a lower limit on the black hole masses, and sub-Eddington accretion would imply larger black holes. However, an average black hole mass ~ 50 times higher is needed to reconcile our data at the characteristic stellar mass of the SMGs, $\sim 10^{11}\ M_\odot$. This would require $\eta \sim 0.02$, which is low given the gas-rich environments in which the SMBHs are likely to reside. Although we do not know the Eddington rate of these galaxies, the large fraction of SMGs that host AGN activity suggests that the accretion is likely to be reasonably efficient (see Alexander et al. 2005a). There is tangential support for this claim from studies that have estimated black hole masses for other active high-redshift populations independently of the Eddington rate, finding $\eta \sim 0.1$–1.7 (e.g., Marconi et al. 2004; McLure & Dunlop 2004; Barger et al. 2000). At the smallest accretion efficiencies found in these studies, the black hole masses would still be ~ 5 times too small for our estimated stellar masses.

There is further support for Eddington-limited or near–Eddington-limited accretion from the similarity between the optical/near-infrared spectra of some SMGs and those of local narrow-line Seyfert 1 (NLS1) galaxies (Ivison et al. 1998; Vernet & Cimatti 2001; Ledlow et al. 2002; Smail et al. 2003; Dawson et al. 2003; Swinbank et al. 2004, 2005; see § 4.3 of Alexander et al. 2005b). If the spectral similarities of the AGN signatures in these two populations are suggestive of comparable physical conditions in the accretion disk around the SMBH, then the approximately Eddington-limited rates estimated for local NLS1 galaxies may be appropriate for SMGs (e.g., Boroson 2002; Collin & Kawaguchi 2004). Moreover, NLS1s appear to have smaller black holes than those predicted from the local M_*-$M_{\rm BH}$ relation; using reverberation mapping, Grupe & Mathur (2004) and Botte et al. (2004) show that the SMBHs in NLS1s are an order of magnitude smaller than predicted for galaxies having a stellar mass of $10^{11}\ M_\odot$. Thus physical models for the accretion disks and SMBHs in NLS1s may be very relevant for understanding the growth of SMBHs in massive, young galaxies at high redshifts.

We do caution the reader that the broad-line region in SMGs may be missed due to heavy extinction in these dusty galaxies, and hence that the spectra may be dominated by a less obscured narrow-line region. High signal-to-noise spectra would be useful to search for faint, broad wings that may be otherwise missed.

There is also theoretical support for $\eta \sim 1$ efficiencies: Granato et al. (2004) and Kawakatu et al. (2003) predict that this condition will be met near the peak epoch of star formation, where these objects have a stronger chance of being detected at submillimeter wavelengths. Interestingly, these models also predict black hole masses ≈ 1–2 orders of magnitude smaller than the local relation during the obscured, starbursting phase, similar to what our data suggest. Hence, while the assumption of Eddington-limited accretion is a large one, it is not a unreasonable choice. We reiterate that even an efficiency 10 times smaller would still result in the black holes in SMGs being smaller than would be predicted by the local relation.

Another uncertainty in the SMBH estimates comes from the bolometric correction applied to the X-ray luminosities. Alexander et al. (2005a) assumed that $6^{+12}_{-4}\%$ of the energy output due to accretion was emitted in the X-ray wave band (Elvis et al. 1994), but if this was lower, the inferred mass of the SMBH would rise. However, they also pointed out that this correction is similar to the estimated bolometric corrections for obscured and unobscured AGNs of similar luminosity to the AGNs in the SMGs (see Alexander et al. 2005a).

A final potential source of uncertainty in the SMBH masses comes from the possibility that a substantial fraction of the X-ray emission from the SMBH is still obscured at rest-frame energies of ~ 20 keV. For instance, Worsley et al. (2005) find that the *Chandra* 2 Ms exposure of the CDF-N fails to recover approximately 40% of the hard X-ray background. This may in part be hidden within highly obscured type 2 quasars (Martinez-Sansigre et al. 2005), but dusty SMGs also harbor obscured AGNs (and could in some cases be type 2 quasars). Indeed, not all SMGs are detected in the *Chandra* 2 Ms X-ray image and so potentially some fraction of the X-ray emission from the SMBH in this population could be missed from the *Chandra* analysis. In § 3.5 of Alexander et al. (2005b), it is pointed out that while obtaining tight constraints on the obscuring column densities for individual sources is difficult, the agreement between their models and X-ray spectra of SMGs ranked by obscuration class is excellent, suggesting that most of the X-ray emission in these sources is accounted for. If a large fraction of the X-ray emission in SMGs is still absorbed, we will need to wait for the next generation of X-ray observatories to find it.

4.3. *Implications for the Evolutionary History of SMGs*

To summarize the previous two subsections, it is possible to find combinations of the parameters used to estimate the stellar and black hole masses of SMGs that would reconcile them with the local $M_\star$-M_{BH} relation. For example, if we assume a 6% bolometric correction, then we require a combination of a typical SMG age of just ~ 50 Myr and an Eddington efficiency of $\eta \sim 0.1$ to place the high-redshift data on the local relation (Fig. 4). This combination is plausible, and if it is the case then the implication is that the stellar and black hole mass grow simultaneously, with a mass ratio that is similar at high redshift as well as low. However, the need for both low Eddington accretion and a very short lifetime for the SMGs is uncomfortable, and hence we should also explore the possibility that the black holes in SMGs are in fact less massive than expected from their stellar masses and the low-redshift $M_\star$-M_{BH} relation. The following discussion assumes that this is indeed the case.

The theoretical models of Granato et al. (2004) suggest that SMBHs may grow exponentially, taking only a few tens of Myr to mature (Kawakatu et al. 2003; Granato et al. 2004). This is a short enough timescale that SMGs with more evolved SMBHs, which lie on the local relationship, should fall within the redshift range probed by our sample. That we do not see such systems implies that as the black hole rapidly builds up its mass, either it shuts down the star formation that powers the far-infrared luminosities (hence they drop out of the submillimeter samples) or the luminosities become so obscured that they are no longer detected in the X-ray wave band.

The former argument supports a scenario that links the QSO and SMG populations. As the black hole undergoes a rapid buildup of mass, the ensuing strong radiation field strips away the obscuring gas and dust, terminating star formation and eventually allowing the AGN to be visible for a short time as a luminous optical quasar (Sanders et al. 1988; Silk & Rees 1998; Fabian 1999; Di Matteo et al. 2005; Alexander et al. 2005b). The close similarity between the redshift distribution of radio-identified SMGs and QSOs (Chapman et al. 2005) also lends support to this hypothesis, as do the relative space densities of SMGs and QSOs given our estimates of their respective lifetimes (Smail et al. 2004). In addition, recent high-resolution adaptive optics imaging by Kuhlbrodt et al. (2005) has shown that the black hole masses and host galaxy luminosities of $z \sim 2$ quasars are consistent with the local $M_\star$-M_{BH} relation, suggesting that QSOs could be the end product of the rapid growth of SMBHs seen soon after an SMG-like phase. Finally, work by Page et al. (2001, 2004) using SCUBA to measure the rest-frame far-infrared luminosities of unobscured and moderately obscured QSOs at $z \sim 2$ verifies that the former class represents a phase of significant SMBH growth but not bulge growth, while the latter may be a transition phase between the star formation–dominated SMGs and AGN-dominated quasars. Thus, if SMGs are the progenitors of quasars, they *must* lie below the locally determined $M_\star$-M_{BH} relation.

In conclusion, there is good qualitative and quantitative agreement in favor of an evolutionary sequence that connects moderate-mass SMBHs in far-infrared–luminous star-forming galaxies at $z \sim 2$–3 (when most of the spheroid is produced) to subsequent growth of the SMBHs during a short phase as a luminous quasar that results in massive spheroids at the present day that lie on the $M_\star$-M_{BH} relation.

5. CONCLUSION

Using deep *Chandra*, *Spitzer*, and ground-based optical and near-infrared imaging data, we have estimated the stellar and black hole masses for a sample of 13 SMGs with precise spectroscopic redshifts. Our main conclusions are as follows:

1. There is a tentative correlation between the rest-frame near-infrared and X-ray luminosity in this sample of SMGs. The X-ray emission likely arises from accretion of matter onto an SMBH and so can be used to estimate its mass. We find a similar correlation between rest-frame X-ray and *V*-band luminosities, but this exhibits more scatter, suggesting that it is more sensitive to dust and age variations in these young, obscured galaxies.

2. The rest-frame UV/optical/near-infrared SEDs of most of our SMGs are dominated by stellar emission and not light from the AGN, and are well described by either a young burst model or an older galaxy with a more continuous star formation history. In both cases, the derived light-to-mass ratios, and hence stellar mass estimates, are similar.

3. The mean stellar mass for the sample is $\log (M_\star) = 11.4 \pm 0.4$, consistent with H$\alpha$ and CO dynamical mass estimates for

the SMG population. Hence the *Spitzer* observations have shown that these intense star-forming galaxies have a significant stellar population in place at $z \sim 2.2$.

4. We find that SMGs are typically 10 times more massive than typical UV-selected galaxies at similar redshifts.

5. We use the assumption of Eddington-limited accretion to estimate the black hole masses for each galaxy in the sample. We find that for a given stellar mass, the black holes are ~ 50 times less massive than those for spheroids with similar stellar masses in the local universe.

6. In order to determine whether the high-redshift SMGs lie on the local $M_{\star}$-M_{BH} relation, we explore the range of assumptions that are used to estimate both the stellar and black hole masses. We find that most reasonable combinations of parameters lead to lower black hole masses at a fixed stellar mass in SMGs at $z \sim 2$, compared to the low-redshift relation for spheroids.

7. We suggest that the NLS1 galaxies may be a good template for understanding the growth of SMBHs at high redshift. They have spectral properties common with many SMGs and (locally) have black hole masses smaller than predicted for less active spheroids.

8. Our results are consistent with a model in which the SMBHs in SMGs subsequently undergo rapid growth to reach the local $M_{\star}$-M_{BH} relation. Such a phase would most naturally be explained if the SMGs evolved into quasars on their way to becoming luminous, passive ellipticals at the present day.

REFERENCES

Adelberger, K. L., Steidel, C. C., Shapley, A. E., Hunt, M. P., Erb, D. K., Reddy, N. A., & Pettini, M. 2004, ApJ, 607, 226
Alexander, D. M., Smail, I., Bauer, F. E., Chapman, S. C., Blain, A. W., Brandt, W. N., & Ivison, R. J. 2005a, Nature, in press
———. 2005b, ApJ, in press
Alexander, D. M., et al. 2003, AJ, 125, 383
Barger, A. J., Cowie, L. L., & Richards, E. A. 2000, AJ, 119, 2092
Baugh, C. M., Lacey, C. G., Frenk, C. S., Granato, G. L., Silva, L., Bressan, A., Benson, A. J., & Cole, S. 2005, MNRAS, 356, 1191
Benson, A. J., Bower, R. G., Frenk, C. S., Lacey, C. G., Baugh, C. M., & Cole, S. 2003, ApJ, 599, 38
Bertin, E., & Arnouts, S. 1996, A&AS, 117, 393
Blain, A. W., Chapman, S. C., Smail, I., & Ivison, R. 2004, ApJ, 611, 725
Bolzonella, M., Miralles, J.-M., & Pelló, R. 2000, A&A, 363, 476
Boroson, T. A. 2002, ApJ, 565, 78
Borys, C., Scott, D., Chapman, S., Halpern, M., Nandra, K., & Pope, A. 2004, MNRAS, 355, 485
Botte, V., Ciroi, S., Rafanelli, P., & Di Mille, F. 2004, AJ, 127, 3168
Bundy, K., Ellis, R. S., & Conselice, C. J. 2005, ApJ, 625, 621
Calzetti, D., Armus, L., Bohlin, R. C., Kinney, A. L., Koornneef, J., & Storchi-Bergmann, T. 2000, ApJ, 533, 682
Capak, P., et al. 2004, AJ, 127, 180
Cavaliere, A., & Vittorini, V. 2002, ApJ, 570, 114
Chapman, S. C., Blain, A. W., Ivison, R. J., & Smail, I. R. 2003, Nature, 422, 695
Chapman, S. C., Smail, I., Blain, A. W., & Ivison, R. J. 2005, ApJ, in press
Chapman, S. C., Smail, I., Windhorst, R., Muxlow, T., & Ivison, R. J. 2004, ApJ, 611, 732
Collin, S., & Kawaguchi, T. 2004, A&A, 426, 797
Cox, A. N. 2000, Allen's Astrophysical Quantities (4th ed.; New York: AIP)
Dawson, S., McCrady, N., Stern, D., Eckart, M. E., Spinrad, H., Liu, M. C., & Graham, J. R. 2003, AJ, 125, 1236
Di Matteo, T., Springel, V., & Hernquist, L. 2005, Nature, 433, 604
Elvis, M., et al. 1994, ApJS, 95, 1
Erb, D. K., Shapley, A. E., Steidel, C. C., Pettini, M., Adelberger, K. L., Hunt, M. P., Moorwood, A. F. M., & Cuby, J. 2003, ApJ, 591, 101
Fabian, A. C. 1999, MNRAS, 308, L39
Farrah, D., Surace, J. A., Veilleux, S., Sanders, D. B., & Vacca, W. D. 2005, ApJ, 626, 70
Frayer, D. T., Ivison, R. J., Scoville, N. Z., Yun, M., Evans, A. S., Smail, I., Blain, A. W., & Kneib, J.-P. 1998, ApJ, 506, L7
Frayer, D. T., et al. 1999, ApJ, 514, L13
Gebhardt, K., et al. 2000, ApJ, 543, L5
Giavalisco, M., et al. 2004, ApJ, 600, L93
Granato, G. L., De Zotti, G., Silva, L., Bressan, A., & Danese, L. 2004, ApJ, 600, 580
Greve, T. R., Ivison, R. J., Bertoldi, F., Stevens, J. A., Dunlop, J. S., Lutz, D., & Carilli, C. L. 2004, MNRAS, 354, 779
Greve, T. R., et al. 2005, MNRAS, in press
Grupe, D., & Mathur, S. 2004, ApJ, 606, L41
Häring, N., & Rix, H. 2004, ApJ, 604, L89
Ivison, R. J., Smail, I., Le Borgne, J.-F., Blain, A. W., Kneib, J.-P., Bezecourt, J., Kerr, T. H., & Davies, J. K. 1998, MNRAS, 298, 583
Ivison, R. J., et al. 2002, MNRAS, 337, 1

John, T. L. 1988, A&A, 193, 189
Kaspi, S., Smith, P. S., Netzer, H., Maoz, D., Jannuzi, B. T., & Giveon, U. 2000, ApJ, 533, 631
Kawakatu, N., Umemura, M., & Mori, M. 2003, ApJ, 583, 85
Kennicutt, R. C. 1998, ARA&A, 36, 189
Kormendy, J., & Richstone, D. 1995, ARA&A, 33, 581
Kuhlbrodt, B., Orndahl, E., Wisotzki, L., & Jahnke, K. 2005, A&A, submitted
Ledlow, M. J., Smail, I., Owen, F. N., Keel, W. C., Ivison, R. J., & Morrison, G. E. 2002, ApJ, 577, L79
Leitherer, C., et al. 1999, ApJS, 123, 3
Magorrian, J., et al. 1998, AJ, 115, 2285
Maraston, C., et al. 2005, MNRAS, submitted
Marconi, A., & Hunt, L. K. 2003, ApJ, 589, L21
Marconi, A., Risaliti, G., Gilli, R., Hunt, L. K., Maiolino, R., & Salvati, M. 2004, MNRAS, 351, 169
Martinez-Sansigre, A., Rawlings, S., Lacy, M., Fadda, D., Marleau, F. R., Simpson, C., Willott, C. J., & Jarvis, M. J. 2005, Nature, 436, 666
McLure, R. J., & Dunlop, J. S. 2004, MNRAS, 352, 1390
Mihos, J. C., & Hernquist, L. 1994, ApJ, 431, L9
Miller, G. E., & Scalo, J. M. 1979, ApJS, 41, 513
Neri, R., et al. 2003, ApJ, 597, L113
Page, M. J., Stevens, J. A., Ivison, R. J., & Carrera, F. J. 2004, ApJ, 611, L85
Page, M. J., Stevens, J. A., Mittaz, J. P. D., & Carrera, F. J. 2001, Science, 294, 2516
Poggianti, B. M., Bressan, A., & Franceschini, A. 2001, ApJ, 550, 195
Poggianti, B. M., & Wu, H. 2000, ApJ, 529, 157
Salpeter, E. E. 1955, ApJ, 121, 161
Sanders, D. B., Soifer, B. T., Elias, J. H., Madore, B. F., Matthews, K., Neugebauer, G., & Scoville, N. Z. 1988, ApJ, 325, 74
Shapley, A. E., Steidel, C. C., Adelberger, K. L., Dickinson, M., Giavalisco, M., & Pettini, M. 2001, ApJ, 562, 95
Shapley, A. E., Steidel, C. C., Erb, D. K., Reddy, N. A., Adelberger, K. L., Pettini, M., Barmby, P., & Huang, J. 2005, ApJ, 626, 698
Silk, J., & Rees, M. J. 1998, A&A, 331, L1
Simpson, C., & Eisenhardt, P. 1999, PASP, 111, 691
Smail, I., Chapman, S. C., Blain, A. W., & Ivison, R. J. 2004, ApJ, 616, 71
Smail, I., Chapman, S. C., Ivison, R. J., Blain, A. W., Takata, T., Heckman, T. M., Dunlop, J. S., & Sekiguchi, K. 2003, MNRAS, 342, 1185
Smail, I., Ivison, R. J., & Blain, A. W. 1997, ApJ, 490, L5
Smail, I., Ivison, R. J., Blain, A. W., & Kneib, J.-P. 2002, MNRAS, 331, 495
Steidel, C. C., Adelberger, K. L., Shapley, A. E., Pettini, M., Dickinson, M., & Giavalisco, M. 2003, ApJ, 592, 728
Steidel, C. C., Shapley, A. E., Pettini, M., Adelberger, K. L., Erb, D. K., Reddy, N. A., & Hunt, M. P. 2004, ApJ, 604, 534
Swinbank, A. M., Smail, I., Chapman, S. C., Blain, A. W., Ivison, R. J., & Keel, W. C. 2004, ApJ, 617, 64
Swinbank, A. M., et al. 2005, MNRAS, 359, 401
Vernet, J., & Cimatti, A. 2001, A&A, 380, 409
Wandel, A., Peterson, B. M., & Malkan, M. A. 1999, ApJ, 526, 579
Wang, W.-H., Cowie, L. L., & Barger, A. J. 2004, ApJ, 613, 655
Webb, T. M., et al. 2003, ApJ, 587, 41
Worsley, M. A., et al. 2005, MNRAS, 357, 1281